Journal of the Korean Nuclear Society
Volume 28, Number 1, February 1996

The Unsteady 2-D Numerical Analysis in a Horizontal Pipe with Thermal Stratification Phenomena

Hag-Ki Youm and Man-Heung Park
Korea Power Engineering Company, Inc.

Sang-Nung Kim
Kyung-Hee University
(Received August 8, 1995)

열성층현상이 존재하는 수평배관내에서의 비정상 2차원 수치해석

염학기 · 박만홍
한국전력기술(주)

김상녕
경희대학교
(1995. 8. 8 접수)

Abstract

In this paper, an unsteady analytical model for the thermal stratification in the pressurizer surge line of PWR plant has been proposed to investigate the temperature profile, flow characteristics, and thermal stress in the pipe. In this model, the interface level, between hot and cold fluid, is assumed to be a function of time while the other models had developed for time independent or steady state. The dimensionless governing equations are solved by using a SIMPLE (Semi-Implicit Method for Pressure Linked Equations) algorithm. The analysis result for an example shows that the maximum dimensionless temperature difference is about 0.78 between hot and cold sections of pipe wall and the maximum thermal stress by thermal stratification is calculated about 276 MPa at the dimensionless time 27.0 under given conditions.

요 약

본 논문에서는, 가압경수로 발전소의 가압기 밀림관내 비정상상태의 열성층현상에 대한 계산 모델을 제안하여 배관내의 온도분포, 유동특성 및 열응력에 대해 연구하였다. 경계면이 시간에 따라 변화가 없거나 정상상태에서 개발된 다른 모델과는 달리 본 모델에서는 고온 및 저온유체 사이의 경계면을 시간의 함수로 가정하였다. 열성층현상에 대한 무차원지배방정식은 SIMPLE 알고리즘을 사용하여 해를 구하였다. 본 수치계산의 결과는 주어진 조건하에서 무차원시간이 약 27.0 일 때 배관의 고온부 및 저온부사이의 최대무차원온도차는 0.78 정도이었고, 이때의 열성층 현상에 의한 최대 열응력은 276 MPa로 계산되었다.

1. Introduction

Thermal stratification and striping phenomena are reported to occur in the piping system of nuclear power plants. These phenomena are usually observed in the pipe line of the safety related systems and may be identified as the source of fatigue damage in the piping system due to the thermal stress loadings which are associated with plant operation modes. The potential for the thermal stratification is the greatest during heatup and cooldown conditions because of the largest temperature difference between the pressurizer and hot leg of PWR (Pressurized Water Reactor) plant.

NRC Bulletin 88-11[1] reported that the phenomena of thermal stratification played an important role in the integrity of pipe because the unexpected motions and the unnegligible thermal stresses occurred in the surge line of PWR plant. Thus the thermal stresses due to the stratification have been considered by the utilities and vendors for the design and licensing processes of the piping[2, 3, 4]. In the view of the thermal stresses in pipes, the temperature change in the fluid region due to the thermal stratification produces at an axial and a circumferential direction in the pipe. Recently, these pipes in the PWR have generally been designed using results of simple analyses, experiments or monitoring[5, 6, 7].

W.R. Smith et al.[8] presented an analytical solution for the steady state temperature distribution in a pipe wall subjected to internally stratified flow. They employed a pin model to determine the wall temperature. V.K. Dhir et al.[9] studied a one dimensional model for prediction of the stratification in a horizontal pipe subjected to fluid temperature transient at inlet. They showed that the propensity of stratification is a function of Richardson number and length of the pipe. Also, J.S. Ann[10] computed the heat transfer rate at the pipe surface using the steady two-dimensional model. P.L. Viollet[11] studied the experiment and numerical modelling of the density effects following a change in the inlet temperature using the unsteady two-dimensional model.

The thermal stratification depends on Richardson number(Ri) defined by the ratio of the buoyancy forces to the inertia forces. If this number is greater than 1, the thermal stratification can be expected to occur. The buoyant force is caused by the density difference between the hot and cold fluid and its magnitude is related to the temperature difference. Therefore, the thermal stratification is likely to occur when the flow velocity is small and the temperature difference is large. The fluctuation of interface level, called thermal striping, is accompanied with thermal stratification, and produces a local stress in the pipe[3, 5]. However, since the thermal striping amplitude is usually very small, it is often assumed that this is not considered in the analysis.

So far, many researches have not accounted the effects on the unsteady thermal stratification in the horizontal pipe. Based on this fact, in this study, the unsteady numerical analysis model is proposed to estimate the heat transfer and flow characteristics with time when the thermal stratification in the horizontal pipe of a pressurizer surge line occurs by outsurge during heatup. Using the given model, the time-dependent temperature profiles in the fluid and pipe wall are calculated with the thermal stratification occurring in the horizontal section of the pipe. Also, the corresponding thermal stresses due to the thermal stratification are presented for the pipe.

2. Model Formulation

Fig.1(a) shows the heatup conditions of the pressurizer surge line. Since the thermal and hydrodynamic conditions are symmetrical with respect to the vertical center line, the half of pipe section has been considered to be a calculation domain as shown Fig.1(b).

In order to solve the governing equations, the following assumptions were made.

- The flow of hot and cold fluid is two-dimensional.
- The properties of fluid and solid except density

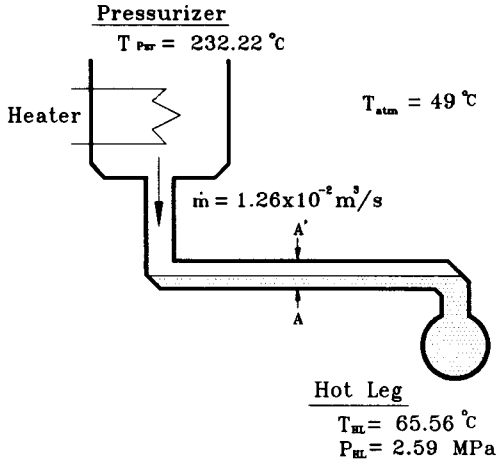

(a) Conditions of the Analysis Model

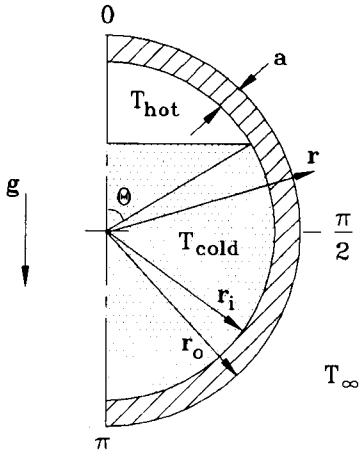

(b) Schematic Diagram of the Calculation Domain

Fig. 1. The Heatup Conditions and Calculation Domain

appearing in body force term are treated as constant.

- The compressibility effects, viscous dissipation and radiation heat transfer of fluids are negligible.
- The thickness of interface layer is neglected, but the interface level is existed.
- The interface level is changed only from top to center of the piping with time when the hot fluid with constant low velocity flows into a upper region of the stagnant cold fluid.

The following dimensionless governing equations for an unsteady two-dimensional flow are as follows [10, 11];

$$\frac{1}{r}\frac{\partial}{\partial r}(ru)+\frac{1}{r}\frac{\partial}{\partial\theta}(v) = 0 \tag{1}$$

$$\frac{\partial v}{\partial t} + \frac{1}{r}\frac{\partial}{\partial r}(ruv) + \frac{1}{r}\frac{\partial}{\partial\theta}(v^2) = -\frac{1}{r}\frac{\partial P}{\partial\theta} + C_1\left\{\frac{1}{r}\frac{\partial}{\partial r}\left(r\frac{\partial v}{\partial r}\right) + \frac{1}{r}\frac{\partial}{\partial\theta}\left(\frac{1}{r}\frac{\partial v}{\partial\theta}\right) - \frac{v}{r^2} + \frac{2}{r^2}\frac{\partial u}{\partial\theta}\right\} - \frac{uv}{r} - \frac{Gr}{Re^2}T\sin\theta \tag{2}$$

$$\frac{\partial u}{\partial t} + \frac{1}{r}\frac{\partial}{\partial r}(ru^2) + \frac{1}{r}\frac{\partial}{\partial\theta}(uv) = -\frac{\partial P}{\partial r} + C_1\left\{\frac{1}{r}\frac{\partial}{\partial r}\left(r\frac{\partial u}{\partial r}\right) + \frac{1}{r}\frac{\partial}{\partial\theta}\left(\frac{1}{r}\frac{\partial u}{\partial\theta}\right) - \frac{u}{r^2} - \frac{2}{r^2}\frac{\partial v}{\partial\theta}\right\} + \frac{v^2}{r} + \frac{Gr}{Re^2}T\cos\theta \tag{3}$$

$$\frac{\partial T}{\partial t} + \frac{1}{r}\frac{\partial}{\partial r}(ruT) + \frac{1}{r}\frac{\partial}{\partial\theta}(vT) = C_2\left\{\frac{1}{r}\frac{\partial}{\partial r}\left(r\frac{\partial T}{\partial r}\right) + \frac{1}{r}\frac{\partial}{\partial\theta}\left(\frac{1}{r}\frac{\partial T}{\partial\theta}\right)\right\} \tag{4}$$

Dimensionless variables are defined as follows;

$$r=\frac{r^*}{r_i^*},\quad a=\frac{(r_o^*-r_i^*)}{r_i^*},\quad v=\frac{v^*}{U_0},$$

$$u=\frac{u^*}{U_0},\quad t=\frac{t^*U_0}{r_i^*},\quad T=\frac{T^*-T^*_{cold}}{T^*_{hot}-T^*_{cold}},$$

$$\mathrm{Pr}=\frac{Cp_f\mu}{k_f},\quad Re=\frac{U_0 r_i^*}{\nu},$$

$$Gr=\frac{g\beta r_i^{*3}(T^*_{hot}-T^*_{cold})}{\nu^2}$$

$$Bi=\frac{h(r_o^*-r_i^*)}{k_s},\quad P=\frac{P^*}{\rho_f U_0^{\,2}},$$

$$P^*=p^*+\rho_f g r^*\cos\theta,$$

$$a_s = \frac{k_s}{\rho_s C p_s}, \quad a_f = \frac{k_f}{\rho_f C p_f} \tag{5}$$

where U_0 is the constant velocity in the axial direction. Although the fluid flow are assumed to be the two-dimensional flow, the axial velocity(U_0) is used to define dimensionless parameter, Richardson number, $Ri(=Gr/Re^2)$. Also, C_1 and C_2 in the equation (2), (3) and (4) represent the diffusion coefficient in the momentum equations and the energy equation, respectively.

$$C_1 = \begin{cases} \frac{1}{Re} & \textit{at fluid} \\ \infty & \textit{at solid} \end{cases} \tag{6}$$

$$C_2 = \begin{cases} \frac{1}{\Pr Re} & \textit{at fluid} \\ \frac{a_s/a_f}{\Pr Re} & \textit{at solid} \end{cases} \tag{7}$$

The initial and boundary conditions for our model are as follows;

$\underline{t=0:}$

$$0 \le r < 1+a \quad \text{and} \quad 0 \le \theta \le \pi ;$$
$$u = v = 0, \qquad T = 0 \tag{8}$$

$\underline{t>0:}$

$$0 \le r \le 1+a \text{ and } \theta = 0 \text{ or } \pi ;$$
$$v = \frac{\partial u}{\partial \theta} = \frac{\partial T}{\partial \theta} = 0 \tag{9}$$

$$0 \le \theta \le \pi \text{ and}$$
$$1 \le r \le 1+a ; \; u = v = 0 \tag{10}$$

$$r = 1+a ; \; \frac{\partial T}{\partial r} = -\frac{Bi(T_o - T_\infty)}{a} \tag{11}$$

$$r = 1 ; \; k_f \frac{\partial T_f}{\partial r} = k_s \frac{\partial T_s}{\partial r} \tag{12}$$

3. Numerical Analysis

The governing equations are a form of non-linear partial differential equation. The discretized governing equations may be derived by the control volume formulation method. The discretization equations have finally a generalized in a form on a grid point P.

$$a_p \phi_p = \Sigma a_{nb} \phi_{nb} + b \tag{13}$$

where ϕ denotes u, v or T, and subscript nb denotes the neighbor grid points of P.

The discretization equations have been solved by a finite volume calculation procedure called SIMPLE (Semi-Implicit Method for Pressure Linked Equations) algorithm, the power law scheme, and TDMA (Tri-Diagonal Matrix Algorithm) using the line-by-line method[12].

The preliminary tests for the number of grid system and time step, t, were carried out, and then we determined an optimal grid system($r \times \theta = 52 \times 32$) as shown Fig. 2, and two optimal time step. A grid spacing in the θ-direction gets wider and wider with the increase of the angle, but that in the r-direction is divided into three regions. Each of the regions in the r-direction is uniformly arranged. However, we give dense nodes near the interface of fluid and pipe, because the velocity and the temperature fields at interface of fluid and pipe are very important to investigate the thermal stratification.

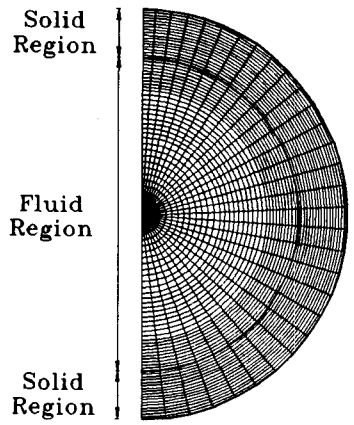

Fig. 2. Grid System of Calculation Domain

The dimensionless time step, t, was employed 0.003 until the first dimensionless time 30 because the characteristics of temperature and flow have been changed to be large. However, it increases to 0.015 after that time to reduce to the calculation time. In order to improve convergence, the relaxation factors of velocity, pressure and temperature are 0.08, 0.08 and 0.15 by dimensionless times 10, and they are 0.35, 0.35 and 0.55 on and after this time, respectively.

The number of iterations is about 200 at the initial step, but it decreases with time. The converged solution was obtained when the error of energy balance was less than 0.01% and the errors of each variables were as follows;

$$\left|\frac{\phi^{m+1}-\phi^{m}}{\phi^{m}}\right| < 10^{-3} \qquad (14)$$

The calculated results are compared with the measured values of a TEMR (T33.19) Test[6] to verify the program. This comparison is showed in Fig. 3. The general agreement between this calculated and measured values is good except small discrepancies near the interface. These discrepancies are probably due to the following facts;

(a) analytical model does not include the interface fluctuation,

(b) the thermal mixing between the hot and cold water is not considered during the insurge time of hot water to the pipe line.

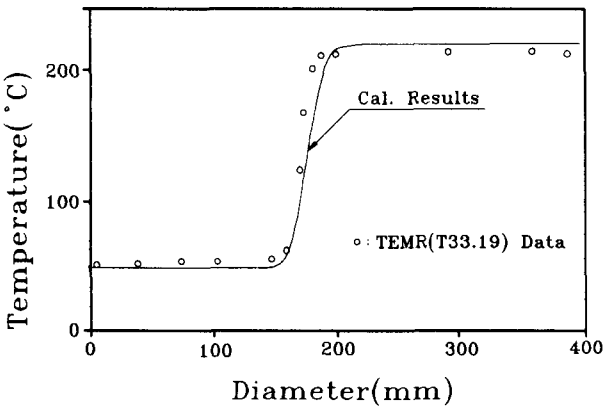

Fig. 3. The Comparison between Our Results and a TEMR Experiment[6]

4. Result and Discussion

Before plant heatup, the reactor coolant loops and pressurizer are filled completely a coolant. During at plant heatup, heaters are on and one reactor coolant system is operated to assist in venting operations. For the this time interval, the reactor coolant system is pressurized to 29 kg_f/cm^2 and heated to 49°C, however, the pressurizer is heated to 216°C and pressurized above the 29kg_f/cm^2. Therefore, the coolant in pressurizer is flowed through the surge line to the reactor coolant loops and the thermal stratification occurs in the horizontal section of surge line as Fig.1(a). And, considering the volume of surge line and the volume flow rate of out-surge, the calculated duration that interface level reaches from $\theta=0$ to the $\theta=\pi/2$(Fig.1(b)) is a dimensionless time 8.58 under the given condition and assumptions.

The design specification of surge line for the numerical analysis is shown in the Table 1, in which the heat transfer coefficient is for the insulated pipe. All properties are calculated by the harmonic mean temperature of cold and hot fluid.

Under the above condition, the dimensionless variables are $Gr=1.9\times10^{10}$, $Re=1.52\times10^{3}$, $Pr=2.2303$, and $Bi=1.57\times10^{-3}$, and the other variables are $T\infty=-3.6\times10^{-2}$, $a=0.222$, $a_s/a_f=25.3$ and $k_s/k_f=23.6$. In this study, the numerical analysis was carried out for the above conditions

Table 1. Design Spec. of Pressurizer Surge Line

Properties & spec.	Value
I.D of pipe	0.27m
Thickness of pipe	0.03m
Material of pipe	SA-312-TP-347
Conductivity	15.8W/m°C
Heat transfer coef.	0.79W/m^2°C
Ambient temp.	43.0°C

4.1. Distribution of Flow and Temperature

Fig. 4(a), (b), and (c) show the distribution of streamlines and isotherms at dimensionless time 3.0, 6.0 and 8. 58, respectively. When by the out surge at heatup the hot fluid with low velocity flows into a stagnant cold fluid, the interface level varies with time from $\theta=0$ to $\theta=\pi/2$ and maintains constant level on and after dimensionless time 8.58. The bracket in the Fig. 4 denotes [maximum value (interval) minimum value] of isothermal distribution.

These isotherms are concentrated in a near region of interface layer, because the hot fluid flows slow in the stagnant cold fluid until dimensionless time 8.58 and the heat transfer between two fluids occurs very large. At these time, so far, the temperature of the lower section of pipe walls corresponds to temperature of cold fluid. And because of the heat transfer between hot fluid and the pipe wall, the temperature difference between inner and outer wall of pipe only occurs in the upper section of the pipe wall. Also, potential of streamlines in the hot region are greater than those of cold region, since the hot fluid flows in the pipe until dimensionless time 8.58.

At dimensionless time 13.5, 27.0, and 54.0, the distributions of streamlines and isotherms are shown in Fig. 4(d), (e), and (f). The profile of isotherms near of interface layer leads to change a typical temperature distribution of thermal stratification, because the natural convection actively occurs in the pipe. As a result, the temperature difference between the inner and outer surfaces of the pipe decreases, and the distribution of flow become stable.

At dimensionless time 108.0, 216.0 and 450.0, the distribution of streamlines and isotherms are shown in Fig. 4(g), (h), and (i). Corresponding to the natural convection in the pipe, the temperature difference between two fluids is small, and the streamline is more stabilized.

Fig. 5 shows the dimensionless temperature distributions in the middle region of the fluid and the pipe inner surface at $\theta=0$, $\pi/3$, $2\pi/3$ and π. Because the temperature distribution of an outer wall similar to these of inner wall except initial state, the temperature distribution of an inner surface of the pipe only is shown.

The dimensionless temperature of the pipe wall at $\theta=0$ rapidly increases until dimensionless time 27.0,

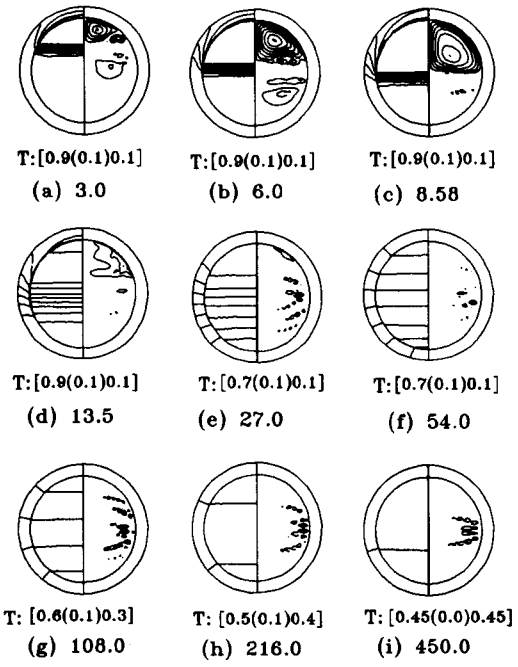

Fig. 4. The Distribution of Isotherms(left) and Streamlines(right) with Time

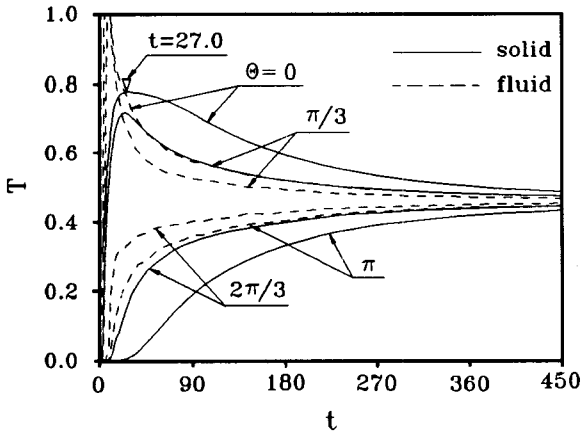

Fig. 5. The Dimensionless Temperature Distribution at Each Region with Time

Table 2. Dimensionless Temp. and ΔT at Each Region

	Time	$\theta=0$	$\theta=\pi$	ΔT
Outer	8.58	0.5	0.0	0.5
wall of	27.0	0.773	5.89×10^{-3}	0.773
pipe	450.0	0.486	0.431	0.055
Inner	8.58	0.664	0.0	0.664
wall of	27.0	0.778	6.60×10^{-3}	0.778
pipe	450.0	0.486	0.431	0.055
Middle	8.58	1.0	1.18×10^{-2}	1.0
region	27.0	0.750	0.223	0.527
of fluid	450.0	0.473	0.445	0.028

but it varies slowly after this time. At $\theta=\pi$, however, it slowly increases until dimensionless time 27.0. Until dimensionless time 15.0, the dimensionless temperatures of fluids rapidly decrease at $\theta=0$ and $\theta=\pi/3$, but they increase at $\theta=2\pi/3$ and $\theta=\pi$. The hot and cold fluids are thermally mixed by natural convection in the pipe with time, and the dimensionless mean temperature of fluid will be about 0.46 for the steady state.

The dimensionless temperatures and the temperature differences between an outer and inner surfaces of the pipe are shown in Table 2.

The maximum dimensionless temperature difference of the pipe wall is computed about 0.78 at dimensionless time 27.0 under the given conditions. Therefore, at this time the maximum thermal stress in pipe by thermal stratification can be predicted. The dimensionless temperature difference of inner wall has somewhat greater than that of outer wall.

4.2. Heat Transfer

To analyze the heat transfer, the local and mean Nusselt numbers along the inner surface of pipe, Nu and $\overline{Nu}$ are defined

$$Nu=\frac{hr_i^*}{k_f}=-\frac{dT}{dr}\Big|_{r=r_i} \tag{15}$$

$$\overline{Nu}=\frac{\bar{h}r_i^*}{k_f}=\frac{1}{\pi}\int_0^{\pi} Nu\,d\theta \tag{16}$$

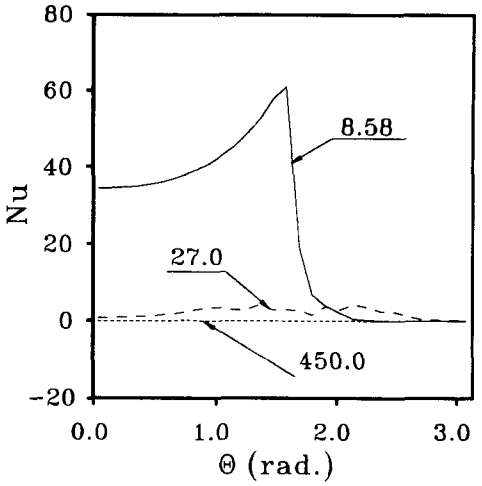

Fig. 6. The Local Nusselt Number along the Inner Wall of Pipe

The local Nusselt number along the inner of pipe is shown at dimensionless time 8.58, 27.0 and 450.0 in Fig. 6.

Since, at dimensionless time 8.58, the temperature difference between the hot fluid and the pipe wall is large, the local Nusselt number in the upper section of pipe is also large. However, it rapidly decreases near the region of interface level since the pipe wall in this region is affected by the cold fluid until this time. At dimensionless time 27.0 as quasi-steady state, the local Nusselt number by the thermal mixture between two fluids is very small and is constant at dimensionless time 450.0.

Fig. 7 shows the mean Nusselt number with time. Until dimensionless time 8.58, the mean heat transfer rate increases since temperature difference between fluid and inner wall of pipe is large. However, during dimensionless time 8.58~27.0, the decrease of the temperature difference between fluid and inner wall of pipe lead to rapidly decrease $\overline{Nu}$. After dimensionless time 27.0, it has been calculated to be almost constant.

4.3. Thermal Stresses

Because the TEMR tests[6] result in that the meas-

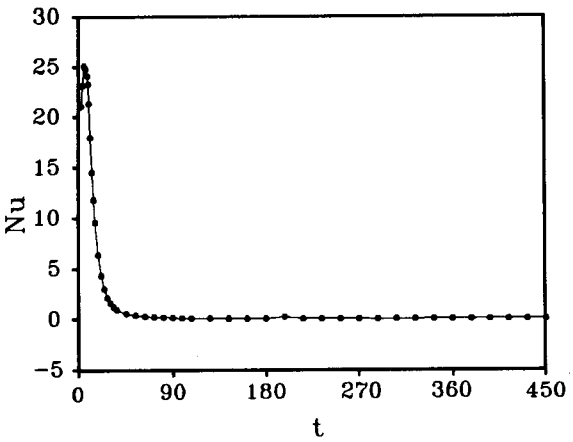

Fig. 7. The Mean Nusselt Number with Time

ured circumferential stresses due to the thermal stratification are small compared to the axial ones, the only axial stresses are considered. In case of an infinitesimal mixing layer height and small wall thickness, the axial stresses are independent of the diameter and the thickness of the pipe. Therefore, the thermal stresses due to the thermal stratification evaluated using the simple calculation method[5] as follow;

When the pipe cannot bend, the membrane stresses in the cold($\Theta > \theta$) and hot ($\Theta < \theta$) regions of a cross section can be calculated by the following equations.

$$\sigma_h = \left(\frac{\Theta}{180^0}\right) \beta \Delta T E \tag{15}$$

$$\sigma_c = -\left(1 - \frac{\Theta}{180^0}\right) \beta \Delta T E \tag{16}$$

And, in case of flexible supports, an additional linear bending stresses due to the thermal stratification are given as follow equation.

$$\sigma_b = 2 \sin \frac{\Theta}{\pi} \beta \Delta T E \cos \theta \tag{17}$$

Under given conditions and assumptions, at the dimensionless time 27.0, the maximum thermal stresses that are the sum of the membrane and bending stresses are each calculated about 276 MPa (40.04 ksi) at the top and the bottom of pipe inner surfaces.

5. Conclusions

The unsteady phenomena of thermal stratification have been numerically investigated in horizontal surge line pipe which connects the pressurizer with the hot leg of reactor coolant system. From this study, we obtain the following conclusions.

1. The complex flow in the upper region and large temperature difference between the inner and outer pipe walls occur until dimensionless time 8.58 when the interface level changes.
2. At dimensionless time 27.0, the maximum dimensionless temperature difference is about 0.78 between the upper and lower section of inner pipe wall surface. At the time, the maximum thermal stress by thermal stratification is calculated about 276 MPa.
3. After dimensionless time 450.0 the thermal stratification is decayed out by the thermal mixture between the hot and cold fluids or fluid and pipe.
4. At dimensionless time 8.58, the maximum local Nusselt number occurs near interface layer, and the maximum mean Nusselt number is obtained.

Nomenclature

a	thickness rate of pipe
Bi	Biot number
C_1, C_2	diffusion coefficient
C_p	specific heat of constant pressure
E	Young's modulus
g	acceleration of gravity
Gr	Grashof number
h	heat transfer coefficient
k	thermal conductivity
$\dot{m}$	mass flow rate
Nu	Nusselt number
P	pressure
Pr	Prandtl number
r, θ	polar coordinate
Re	Reynolds number
Ri	Richardson number
T	temperature

t	time
U_0	velocity of z direction
u, v	velocity of r and θ direction
α	thermal diffusivity
β	coefficient of thermal expansion
Θ	angle between the top and the interface
σ	stress
ϕ	general dependent variable
ρ	density
μ	viscosity

Superscript

m	iteration number
*	physical quantity
$-$	mean value

Subscript

b	bending
f, s	fluid and solid region
HL	Hot Leg
$hot, cold$	hot and cold region of fluid
i, o	inside and outside
nb	neighbor grid point
pz	Pressurizer
∞	ambient

References

1. NRC, "Pressurizer Surge Line Thermal Stratification", NRC Bulletin No. 88-11 (1988)
2. Shah, V.N. and MacDonald, P.E. "Residual Life Assesment of Major Light Water Reactor Components-Overview Volume 1", NUREG/CR-4731 EGG-2469 Vol. 1, pp 46~62 (1989)
3. Kim, J.H Ridt, R.M. and Deardorff, A.F. "Thermal Stratification and Reactor Piping Integrity", Nuclear Engineering and Design, Vol. 139, pp. 83~95 (1993)
4. Ensel, C., Colas, A. and Barthez, "Stress Analysis of a 900MW Pressurizer Surge Line Including Stratification Effect", Nuclear Engineering and Design, Vol. 153, pp. 197~203 (1995)
5. Talja, A. and Hansjosten, E. "Result of Thermal Stratification Test in a Horizontal Pipe Line at the HDR-Facility", Nuclear Engineering and Design, Vol. 118, pp. 29~41 (1990)
6. Wolf, L., Häfner, W., Geiss, M., Hanjosten, E. and Katzenmeiner, G. "Result of HDR-Experiments for Pipe Load under Thermally Stratified Flow Conditions", Nuclear Engineering and Design, Vol. 137, pp. 387~404 (1992)
7. Guyette, M., "Prediction of Fluid Temperatures from Measurements of Outside Wall Temperatures in Pipe", Journal of Pressure Vessel Technology, Vol. 116, pp. 179~187 (1994)
8. Simth, W.R., Cassell, D.S. and Schlereth, E.P. "A Solution for the Temperature Distribution in a Pipe wall Subjected to Internally Stratified Flow", Proceeding of the 1988 Joint ASME-ANS Nuclear Power Conference, pp. 45-50 (1988)
9. Dhir, V.K., Amar, R.C. and Mills, J.C. "A Dimensional Model for the Prediction of Stratification in Horizontal Pipes Subjected to Fluid Temperature Transient at Inlet; Part1 : Hydrodynamic Model and Part2 : Thermal Model", Nuclear Engineering and Design, Vol. 107, pp. 307-325 (1988)
10. Ann, J.S., "A Numerical Study on the Natural Convection in a Horizontal Pipe with Thermal Stratification", Promotion Report, KAERI (1993)
11. Viollet, P.L., "Observation and Numerical Modelling of Density Currents Resulting from Thermal Transients in a Non Rectilinear Pipe", J. of Hydraulic Research, Vol. 25, No. 2, pp. 235-261 (1987)
12. Patankar, S.V., "Numerical Heat Transfer and Fluid Flow", McGraw-Hill Book Company (1980)